SEISMIC ANALYSIS OF IN-PLANE LOADED WALLS IN UNREINFORCED MASONRY BUILDINGS WITH FLEXIBLE DIAPHRAGMS

Yasuto Nakamura[1], Hossein Derakhshan[2], Jason M. Ingham[3], Michael C. Griffith[4]

SUMMARY

It is well recognised that the dynamic response of unreinforced masonry buildings with flexible timber diaphragms typically contains multiple dominant modes associated with the excitations of the diaphragms and the in-plane walls. Existing linear analysis methods for this type of structure commonly account for the multi-mode behaviour by assuming the independent vibrations of the in-plane loaded walls (in-plane walls) and the diaphragms. Specifically, the in-plane walls are considered to be rigid and the unmodified ground motion is assumed to be transmitted up the walls to the diaphragm ends. While this assumption may be appropriate for many low-rise unreinforced masonry buildings, neglecting the dynamic interaction between the diaphragms and the in-plane walls can lead to unreliable predictions of seismic demands. An alternative analysis approach is proposed in this paper, based on the mode properties of a system in which (1) the mass ratios between the diaphragms and the in-plane wall are the same at all levels, and (2) the periods of the diaphragms are the same at all levels. It is proposed that under these conditions, two modes are typically sufficient to obtain the peak seismic demands of the in-plane walls in elastically responding low-rise regular buildings. The applicability of the two-mode analysis approach is assessed for more general diaphragm configurations by sensitivity analysis, and the limitations are identified. The two-mode approach is then used to derive a response modification factor, which may be used in conjunction with a linear static procedure in the seismic assessment of buildings with flexible diaphragms.

INTRODUCTION

In older unreinforced masonry (URM) buildings, the floor and roof diaphragms are often constructed of flexible timber systems. The flexibility of the diaphragms introduce two dynamic effects that are absent in rigid diaphragm structures. Firstly, the non-rigid diaphragms lead to an intermediate coupling of the adjacent in-plane loaded walls (in-plane walls), resulting in a limited distribution of inertial forces amongst the lateral-load resisting elements. Secondly, the excitations of the diaphragms themselves provide feed-back effects on the in-plane walls, potentially modifying the behaviour of the walls. As these older structures are highly vulnerable to seismic action, there is a need for a practical procedure to evaluate the seismic demand imposed on the in-plane walls for the global assessment of URM buildings with flexible diaphragms.

The simplest seismic analysis procedure, and likely the first choice of analysis in practice for typical low-rise regular URM buildings, is the linear static method. In the context of the performance-based assessment guideline of ASCE 41-13 [1], the equivalent static base shear is determined using a corresponding linear system,

$$V = C_1 C_2 C_m S_a W \qquad (1)$$

where V is the elastic base shear, C_1 is a modification factor relating maximum inelastic displacement to the elastic displacement, C_2 expresses the modification for the effect of stiffness and strength degradations, C_m accounts for higher mode mass participation (taken to be 1.0 for URM), S_a is the spectral acceleration at the fundamental period of the structure, and W is the seismic weight of the structure. The elastic base shear in Equation 1 is not the actual base shear that the building would experience, but rather an equivalent force that would induce the expected inelastic displacement on the elastic system [2]. The demand so calculated is compared against the component capacities to ensure,

$$\kappa Q_{CE} \geq Q_{UD}/m \qquad (2)$$

where κ is the knowledge factor, Q_{CE} is the expected component strength (i.e. rocking or shear strength), Q_{UD} is the elastic demand (i.e. moments or shear forces) calculated based on Equation 1. m is the modification factor that accounts for the component ductility for a particular performance level [2].

Several studies have been conducted to incorporate the effect of diaphragm flexibility in the demand estimation (Equation 1) of the linear static procedure. ASCE 41-13 and NZSEE [3] stipulate that the fundamental period of unreinforced masonry buildings of less than six storeys in height, with single-span flexible diaphragms may be calculated as

[1]*PhD student, University of Adelaide, Australia*

[2]*Post-doctural research fellow, University of Adelaide, Australia*

[3]*Professor, University of Auckland, New Zealand*

[4]*Professor. University of Adelaide, Australia*

$$T = \sqrt{3.07\Delta_d} \quad (3)$$

where Δ_d in metres is the maximum diaphragm deformation due to a lateral load of 1.0g. Equation 3 has been shown to be the fundamental period of a fix-ended flexural beam [4]. Therefore, the expression considers the in-plane walls to remain rigid and the diaphragm to vibrate independent of the in-plane walls. An alternative procedure was proposed by Kim and White [5]. In their method, a subassembly consisting of the two adjacent in-plane walls at a given storey and the supported diaphragm is initially separated from the rest of the structure. The peak elastic demand of the subassembly is then determined, considering the subassembly to be subjected to ground acceleration. Hence in this procedure, parts of the structure are assumed to remain rigid for the estimation of demand on each subassembly. The peak forces of the subassemblies are then combined together by direct summation to estimate the peak seismic demand of the actual structure. Recently, Knox [6] proposed a method in which the equivalent seismic force of the in-plane wall and the diaphragms are firstly determined separately. The possible correlations in the responses are subsequently considered through the use of a modal combination rule to obtain the total demand. A set of modification factors similar to Equation 1 was also suggested to account for the inelastic behaviour.

For symmetric (or almost symmetric) structures, the coupling effect of the diaphragms may be considered negligible and the diaphragms can be idealised as single-degree-of-freedom (SDOF) systems mounted on a primary structure (in-plane wall) at floor levels [7, 8]. In this idealisation, the diaphragms can be viewed as heavy secondary systems. It is well recognised that heavy secondary systems have the potential to modify the dynamic behaviour of the primary structure [9], and the response of the primary structure can only be evaluated accurately by considering the dynamics of the combined system. However, the foregoing review of the existing analysis methods incorporating the effects of diaphragm flexibility revealed that the interactions between the in-plane walls and the diaphragms are not explicitly considered. Therefore, the existing methods are strictly applicable when the following two conditions are met:

- the period of the diaphragm is sufficiently larger than the period of the in-plane walls (so that the in-plane walls may be considered as providing essentially rigid support conditions at diaphragm ends); and
- the period of the in-plane walls is sufficiently smaller than the dominant period of the ground motion (so that the important frequency content of the ground motion is not filtered out by the in-plane walls).

For many low-rise unreinforced masonry buildings, these conditions are satisfied. However, there are cases in which they may not be appropriate, including:

- long and narrow buildings with loading perpendicular to the narrow end;
- flexible in-plane walls with large openings; and
- stiffened/retrofitted diaphragms.

This study proposes an alternative, and more rational, method to account for diaphragm flexibility by explicitly considering the interaction between the elastically responding in-plane walls and the diaphragms.

In the first part of the paper, the modal properties of structures with an idealised diaphragm configuration are derived to show that two modes of the combined system are closely related to a given mode of the uncoupled in-plane wall. These two modes are further shown to retain the same proportion of the mass participation as the associated mode of the uncoupled in-plane wall, leading to the concept of the two-mode analysis in capturing the effect of diaphragm flexibility. The applicability of the two-mode analysis for more general diaphragm configurations is evaluated by sensitivity analysis, and the limitation of the approach is identified. In the second part of the paper, the two-mode approach is used to derive an expression for the modification of the peak base shear to account for flexible diaphragms in the context of the linear static method. A numerical validation is provided to demonstrate that the proposed method gives more consistent results in comparison to dynamic analyses than existing procedures for a wide range of diaphragm stiffness.

STRUCTURAL IDEALISATION

It is considered that symmetric, or essentially symmetric, unreinforced masonry buildings with flexible diaphragms can be idealised as planar discrete multi-degree-of-freedom (MDOF) systems as shown in Figure 1. In the idealisation, the out-of-plane walls are assumed to be cracked and their stiffness contributions are neglected, while their masses are appropriately distributed to the diaphragm and in-plane wall degrees of freedom.

Even though the in-plane walls are conceptually represented in a discrete manner, the difficulty associated with the derivation of storey stiffness of perforated walls [10, 11] is avoided in the analysis that follows, by characterising their elastic properties by the uncoupled wall's periods and mode shapes.

The SDOF idealisation of the diaphragm at each level requires the definitions of the equivalent mass and the period. The idealisation adopted in this study follows a similar approach to [12], in which the equivalent SDOF system is constructed such that it produces (1) the same period, and (2) the same total resisting force, of the diaphragm when it deforms in an assumed displacement shape. The first condition has been investigated by [4], who showed that the shear beam idealisation best approximates the deformed shape of single straight-sheathing diaphragms typically found in older URM buildings. By the generalised SDOF analysis [13], the period of the diaphragms deforming in shear has been shown to be

$$T_d = 0.7\sqrt{\frac{W_D L}{G_d B}} \quad (4)$$

where W_D is the total tributary weight of the diaphragm including any tributary weight of the out-of-plane walls, L and B are the dimensions of the diaphragms perpendicular and parallel to the direction of loading respectively, and G_d is the stiffness of the diaphragm. Using the consistent shear beam idealisation, the equivalent mass satisfying the second condition can also be derived by the generalised SDOF analysis as

$$m_d = \frac{126}{155}\frac{W_D}{g} \quad (5)$$

The equivalent SDOF idealisation of the diaphragm is hence defined by Equations 4 and 5 and the equivalent stiffness may also be obtained from these expressions. The mass and the stiffness of the combined structure ($\boldsymbol{m}$ and $\boldsymbol{k}$) can then be written in terms of the uncoupled component matrices, $\boldsymbol{m}_w$ and $\boldsymbol{k}_w$ for the in-plane wall and $\boldsymbol{m}_d$ and $\boldsymbol{k}_d$ for the diaphragms,

$$\boldsymbol{m} = \begin{bmatrix} \boldsymbol{m}_w & \boldsymbol{0} \\ \boldsymbol{0} & \boldsymbol{m}_d \end{bmatrix}, \ \boldsymbol{k} = \begin{bmatrix} \boldsymbol{k}_w + \boldsymbol{k}_d & -\boldsymbol{k}_d \\ -\boldsymbol{k}_d & \boldsymbol{k}_d \end{bmatrix} \quad (6)$$

As an example, for the two-storey model of Figure 1, the uncoupled matrices can be written as

$$\boldsymbol{m}_w = \begin{bmatrix} m_{w1} & 0 \\ 0 & m_{w2} \end{bmatrix},\ \boldsymbol{k}_w = \begin{bmatrix} k_{w1}+k_{w2} & -k_{w2} \\ -k_{w2} & k_{w2} \end{bmatrix}$$

$$\boldsymbol{m}_d = \begin{bmatrix} m_{d1} & 0 \\ 0 & m_{d2} \end{bmatrix},\ \boldsymbol{k}_d = \begin{bmatrix} k_{d1} & 0 \\ 0 & k_{d2} \end{bmatrix} \quad (7)$$

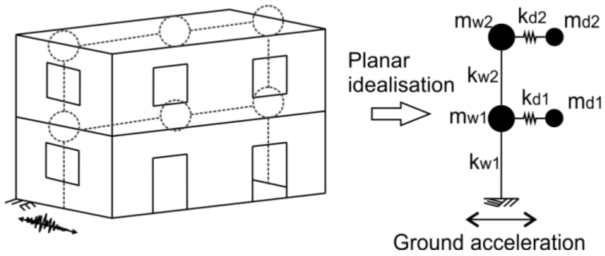

Figure 1: Idealisation of symmetric structures.

MODAL ANALYSIS

Modal Properties of Idealised Diaphragm Configuration

The modal properties of the planar model in Figure 1 can be shown to be functions of the uncoupled in-plane wall's normal modes under a particular diaphragm condition.

Consider the undamped free vibration of the planar model

$$\begin{bmatrix} \boldsymbol{m}_w & \boldsymbol{0} \\ \boldsymbol{0} & \boldsymbol{m}_d \end{bmatrix}\begin{bmatrix} \ddot{\boldsymbol{u}}_w \\ \ddot{\boldsymbol{u}}_d \end{bmatrix} + \left(\begin{bmatrix} \boldsymbol{k}_w & \boldsymbol{0} \\ \boldsymbol{0} & \boldsymbol{0} \end{bmatrix} + \begin{bmatrix} \boldsymbol{k}_d & -\boldsymbol{k}_d \\ -\boldsymbol{k}_d & \boldsymbol{k}_d \end{bmatrix}\right)\begin{bmatrix} \boldsymbol{u}_w \\ \boldsymbol{u}_d \end{bmatrix} = \boldsymbol{0} \quad (8)$$

where $\mathbf{u}_w$ and $\mathbf{u}_d$ are the relative displacement vectors (with respect to the ground) of the in-plane wall and the diaphragms respectively, of size equal to the number of floors. Differentiation with respect to time is denoted by over-script dots. The dynamic properties of the combined structure can be related to the modal properties of the uncoupled components by the transformation [14],

$$\begin{bmatrix} \boldsymbol{u}_w \\ \boldsymbol{u}_d \end{bmatrix} = \begin{bmatrix} \boldsymbol{\Phi}'_w & \boldsymbol{0} \\ \boldsymbol{0} & \boldsymbol{\Phi}'_d \end{bmatrix}\begin{bmatrix} \boldsymbol{q}_w \\ \boldsymbol{q}_d \end{bmatrix} = \boldsymbol{\Lambda}\boldsymbol{q} \quad (9)$$

where the columns of the matrices $\boldsymbol{\Phi}_w'$ and $\boldsymbol{\Phi}_d'$ contain the eigenvectors of the uncoupled in-plane wall and the diaphragms respectively, normalised such that

$$\boldsymbol{\Phi}'^{\mathrm{T}}_w \boldsymbol{m}_w \boldsymbol{\Phi}'_w = \mathbf{I} \quad (10)$$

$$\boldsymbol{\Phi}'^{\mathrm{T}}_d \boldsymbol{m}_d \boldsymbol{\Phi}'_d = \mathbf{I} \quad (11)$$

where $\mathbf{I}$ is the identity matrix. Substituting Equation 9 in Equation 8 and pre-multiplying by $\boldsymbol{\Lambda}^{\mathrm{T}}$ gives

$$\boldsymbol{m}^*\ddot{\boldsymbol{q}} + \boldsymbol{k}^*\boldsymbol{q} = \boldsymbol{0} \quad (12)$$

where

$$\boldsymbol{m}^* = \begin{bmatrix} \boldsymbol{\Phi}'^{\mathrm{T}}_w & \boldsymbol{0} \\ \boldsymbol{0} & \boldsymbol{\Phi}'^{\mathrm{T}}_d \end{bmatrix}\begin{bmatrix} \boldsymbol{m}_w & \boldsymbol{0} \\ \boldsymbol{0} & \boldsymbol{m}_d \end{bmatrix}\begin{bmatrix} \boldsymbol{\Phi}'_w & \boldsymbol{0} \\ \boldsymbol{0} & \boldsymbol{\Phi}'_d \end{bmatrix} = \mathbf{I} \quad (13)$$

$$\boldsymbol{k}^* = \begin{bmatrix} \boldsymbol{\Omega}_w^2 & 0 \\ 0 & 0 \end{bmatrix} + \begin{bmatrix} \boldsymbol{\Phi}'^{\mathrm{T}}_w \boldsymbol{k}_d \boldsymbol{\Phi}'_w & -\boldsymbol{\Phi}'^{\mathrm{T}}_w \boldsymbol{k}_d \boldsymbol{\Phi}'_d \\ -\boldsymbol{\Phi}'^{\mathrm{T}}_d \boldsymbol{k}_d \boldsymbol{\Phi}'_w & \boldsymbol{\Omega}_d^2 \end{bmatrix} \quad (14)$$

The diagonal matrices $\boldsymbol{\Omega}_w$ and $\boldsymbol{\Omega}_d$ contain the modal frequencies of the uncoupled in-plane wall and diaphragms respectively. The eigenvalue problem of the transformed Equation 12 is

$$\left(\boldsymbol{k}^* - \omega_j^2\mathbf{I}\right)\boldsymbol{\phi}_j^* = \boldsymbol{0} \quad (15)$$

where ω_j is the j^{th} frequency and $\boldsymbol{\phi}_j^*$ is the j^{th} mode shape (in the transformed coordinate) of the combined structure. Note that the size of $\boldsymbol{\phi}_j^*$ is twice the number of floor levels as it contains both the in-plane wall's and the diaphragms' degrees of freedom. Closed-form solutions are readily obtained, if the following conditions are imposed on the diaphragms configuration:

- the equivalent mass of the diaphragm at any floor level is a constant fraction R_m of the tributary mass of the in-plane wall at the same level; and
- the periods of the diaphragms are equal at all levels.

These conditions are expressed mathematically as

$$\boldsymbol{m}_d = R_m\boldsymbol{m}_w \quad (16)$$

$$\boldsymbol{\Omega}_d = \omega_d\mathbf{I} \quad (17)$$

By the dynamics of a SDOF system, it also follows that

$$\boldsymbol{k}_d = \omega_d^2\boldsymbol{m}_d \quad (18)$$

By substituting Equations 16 to 18 in Equation 15 and writing out the equations corresponding to the in-plane wall and the diaphragms separately, $\boldsymbol{\phi}_j^* = [\boldsymbol{\phi}_{wj}^*\ \boldsymbol{\phi}_{dj}^*]^{\mathrm{T}}$, yields the following simultaneous equations

$$\left(\boldsymbol{\Omega}_w^2 - \omega_j^2\mathbf{I}\right)\boldsymbol{\phi}_{wj}^* = -\omega_d^2\left(R_m\boldsymbol{\phi}_{wj}^* - \boldsymbol{\Phi}'^{\mathrm{T}}_w\boldsymbol{m}_d\boldsymbol{\Phi}'_d\boldsymbol{\phi}_{dj}^*\right) \quad (19)$$

$$-\omega_j^2\boldsymbol{\phi}_{dj}^* = -\omega_d^2\left(-\boldsymbol{\Phi}'^{\mathrm{T}}_d\boldsymbol{m}_d\boldsymbol{\Phi}'_w\boldsymbol{\phi}_{wj}^* + \boldsymbol{\phi}_{dj}^*\right) \quad (20)$$

Equation 20 can be re-arranged to give the expression for the diaphragms' mode shape in terms of the mode shape of the in-plane wall

$$\boldsymbol{\phi}_{dj}^* = \frac{\omega_d^2}{\omega_d^2-\omega_j^2}\left(\boldsymbol{\Phi}'^{\mathrm{T}}_d\boldsymbol{m}_d\boldsymbol{\Phi}'_w\right)\boldsymbol{\phi}_{wj}^* \quad (21)$$

Substituting Equation 21 in Equation 19 and applying the mass orthonormal condition (Equations 10 and 11) gives a diagonalised equation with the unknowns ω_j and $\boldsymbol{\phi}_{wj}^*$

$$\left[\omega_j^4\mathbf{I} - \omega_j^2\left(\boldsymbol{\Omega}_w^2 + \omega_d^2(1+R_m)\mathbf{I}\right) + \omega_d^2\boldsymbol{\Omega}_w^2\right]\boldsymbol{\phi}_{wj}^* = \boldsymbol{0} \quad (22)$$

For a nontrivial solution,

$$det\left[\omega_j^4\mathbf{I} - \omega_j^2\left(\boldsymbol{\Omega}_w^2 + \omega_d^2(1+R_m)\mathbf{I}\right) + \omega_d^2\boldsymbol{\Omega}_w^2\right] = 0 \quad (23)$$

Because the matrices in Equation 23 are triangular (more specifically, diagonal), the determinant is the product of the diagonal entries [15]. For the determinant to equal zero, each term of the product must equal zero, hence

$$\omega_j^4 - \omega_j^2[\omega_{wn}^2 + \omega_d^2(1+R_m)] + \omega_d^2\omega_{wn}^2 = 0 \quad (24)$$

where ω_{wn} denotes the n^{th} diagonal entry of $\boldsymbol{\Omega}_w$. As Equation 24 is a quadratic in ω_j^2, two solutions exist for ω_j^2 for each n^{th} mode of the uncoupled in-plane wall. Denoting these by $\omega_{n,L}^2$ and $\omega_{n,U}^2$ (L for *lower* and U for *upper* eigenvalues),

$$\omega_{n,L}^2 = \frac{\omega_{wn}^2+\omega_d^2(1+R_m)-\sqrt{\left[\omega_{wn}^2+\omega_d^2(1+R_m)\right]^2-4\omega_d^2\omega_{wn}^2}}{2} \quad (25)$$

$$\omega_{n,U}^2 = \frac{\omega_{wn}^2+\omega_d^2(1+R_m)+\sqrt{\left[\omega_{wn}^2+\omega_d^2(1+R_m)\right]^2-4\omega_d^2\omega_{wn}^2}}{2} \quad (26)$$

Equations 25 and 26 show that two modes of the combined system can be attributed to each mode of the uncoupled in-plane wall. The normal mode of the uncoupled in-plane wall is herein referred to as the "original mode". The two modes of the combined structure attributed to the n^{th} original mode are referred to collectively as the n^{th} "mode pair".

In Figure 2 the frequencies of the mode pair are plotted as normalised to the frequency of the original mode. When the diaphragm is overly flexible, the higher mode approaches the frequency of the uncoupled in-plane wall while the lower mode's frequency tends to zero. In addition, the frequencies of the mode pair become independent of the mass ratio. These observations suggest that the interactions between the diaphragms and the in-plane wall become negligible as the diaphragm becomes completely flexible. Conversely, when the diaphragm is very stiff, the higher mode increases exponentially, while the lower mode approaches a frequency somewhat smaller than that of the uncoupled in-plane wall. This reduction in the lower mode's frequency depends on the mass ratio; in fact, the frequency approaches that of the rigid diaphragm condition, with the reduction in the frequency proportional to $1/\sqrt{(1+R_m)}$.

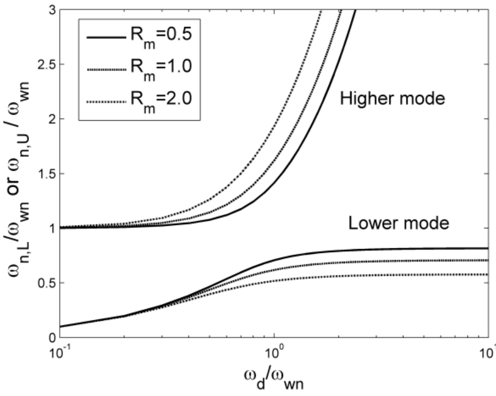

Figure 2: Frequencies of mode pair.

The correspondence between the original mode and the mode pair can be further illustrated by their mode shapes. By substituting Equation 25 or 26 in the transformed Equation 22, it can be seen the standard basis vectors provide the required solution for $\boldsymbol{\phi}_{wn,L}{}^*$ and $\boldsymbol{\phi}_{wn,U}{}^*$

$$\boldsymbol{\phi}^*_{w1,\langle.\rangle} = [1 \quad 0 \cdots]^{\mathrm{T}}, \boldsymbol{\phi}^*_{w2,\langle.\rangle} = [0 \quad 1 \quad 0 \cdots]^{\mathrm{T}}\ etc. \quad (27)$$

To simplify the notation, $\langle.\rangle$ is used to replace the subscripts L or U in the above and the following expressions. Where $\langle.\rangle$ appears multiple times in an equation, they refer to the consistent component (L or U) of the mode pair. Applying the transformation back to the physical coordinate (Equation 9) yields

$$\boldsymbol{\phi}_{wn,\langle.\rangle} = \boldsymbol{\Phi}'_w \boldsymbol{\phi}^*_{wn,\langle.\rangle} = \boldsymbol{\phi}'_{wn} \quad (28)$$

where $\boldsymbol{\phi}_{wn}{}'$ is the n^{th} column vector of $\boldsymbol{\Phi}_w{}'$ and $\boldsymbol{\phi}_{wn,\langle.\rangle}$ is the eigenvector corresponding to the in-plane wall's degree of freedom of the n^{th} mode pair. The expression shows that the in-plane wall's mode shape (of the n^{th} mode pair) is proportional to the original, uncoupled in-plane wall's mode shape. The mode shape of the diaphragms in the n^{th} mode pair can be calculated from Equations 21, 28 and 9 as

$$\boldsymbol{\phi}_{dn,\langle.\rangle} = \frac{\omega_d^2}{\omega_d^2 - \omega_{n,\langle.\rangle}^2} \boldsymbol{\phi}'_{\mathrm{wn}} \quad (29)$$

In this expression, the displacement vector $\boldsymbol{\phi}_{dn,\langle.\rangle}$ is expressed as relative to the ground. Equation 29 also indicates that the mode shapes of the diaphragms are proportional to that of the original mode. Figure 3 shows the plot of the normalised mode shapes of the combined structure. The in-plane wall and the diaphragms are in-phase in the lower mode pair, and are out-of-phase in the higher mode pair.

The properties of the mode pair derived in this section are specific to the diaphragm conditions of Equations 16 and 17. Under these conditions, a correspondence between the mode properties of the combined system and those of the uncoupled in-plane wall has been identified. Specifically, two modes (mode pair) of the combined system arise from each mode of the uncoupled in-plane wall (original mode). The mode shapes of the mode pair are proportional to that of the original mode. The in-plane wall and diaphragms are in-phase in the lower mode pair, and are out-of-phase in the higher mode pair. The significance of the mode pair is described in the next section.

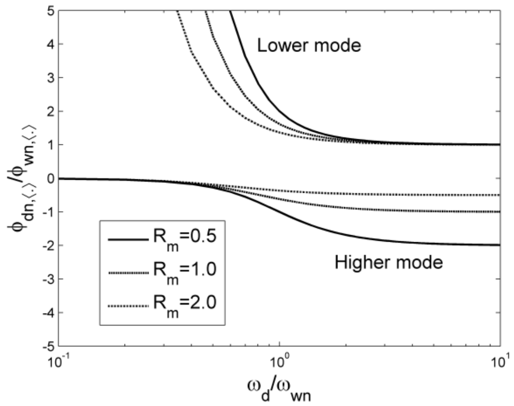

Figure 3: Mode shapes of mode pair.

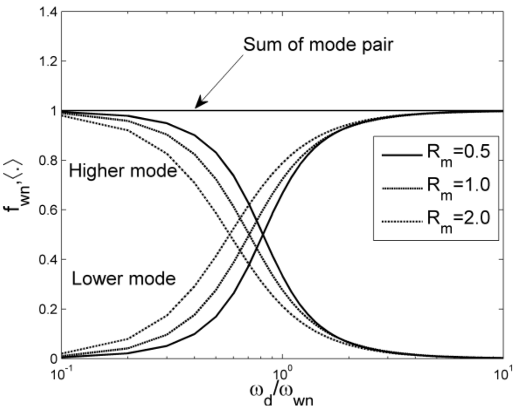

(a) In-plane walls

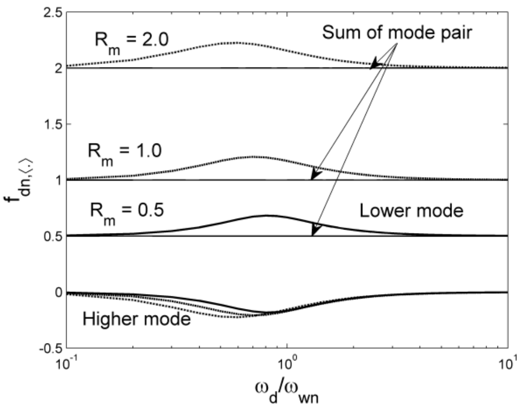

(b) Diaphragms

Figure 4: Scaling factors applied to the equivalent static force of uncoupled in-plane wall.

Significance of Mode Pair for Seismic Analysis

In the seismic analysis of linearly elastic structures, it is usually sufficient to include only the first few modes to calculate the peak response quantities. A common parameter used to determine the number of modes to include, as typically specified in seismic codes, is the proportion of the effective modal mass to the total seismic mass of the structure. The effective modal mass M_n may be obtained as the sum of the effective earthquake force distribution $\boldsymbol{s}_n$ [13].

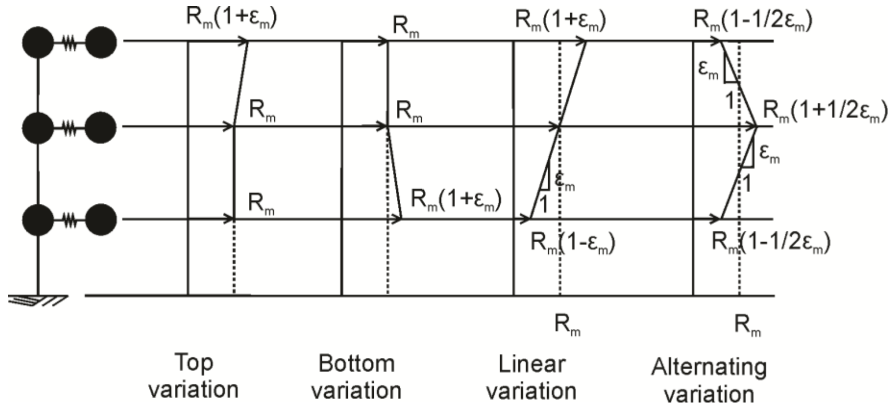

Figure 5: Variation in the reference mass ratio (for variation in reference period, replace Rm by Td and εm by εT).

$$M_n = \mathbf{1}^{\mathrm{T}} \boldsymbol{s}_n \tag{30}$$

where

$$\boldsymbol{s}_n = \Gamma_n \boldsymbol{m}\boldsymbol{\phi}_n = \frac{\boldsymbol{\phi}_n^{\mathrm{T}}\boldsymbol{m}\mathbf{1}}{\boldsymbol{\phi}_n^{\mathrm{T}}\boldsymbol{m}\boldsymbol{\phi}_n}\boldsymbol{m}\boldsymbol{\phi}_n \tag{31}$$

For the diaphragm configuration specified in Equations 16 and 17, Equation 31 for the mode pair can be evaluated as

$$\boldsymbol{s}_{n,\langle.\rangle} = \begin{bmatrix} f_{wn,\langle.\rangle}\boldsymbol{s}_{wn} \\ f_{dn,\langle.\rangle}\boldsymbol{s}_{wn} \end{bmatrix} \tag{32}$$

where $\boldsymbol{s}_{wn}$ is the effective earthquake force distribution of the original mode defined analogously to Equation 31. The coefficients $f_{wn,\langle.\rangle}$ and $f_{dn,\langle.\rangle}$ may be thought of as scaling factors applied to the in-plane wall and the diaphragms respectively,

$$f_{wn,\langle.\rangle} = \frac{1+R_m\left(\frac{\omega_d^2}{\omega_d^2-\omega_{n,\langle.\rangle}^2}\right)}{1+R_m\left(\frac{\omega_d^2}{\omega_d^2-\omega_{n,\langle.\rangle}^2}\right)^2},$$

$$f_{dn,\langle.\rangle} = R_m\left(\frac{\omega_d^2}{\omega_d^2-\omega_{n,\langle.\rangle}^2}\right) f_{wn,\langle.\rangle} \tag{33}$$

The plots of $f_{wn,\langle.\rangle}$ and $f_{dn,\langle.\rangle}$ are shown in Figure 4 for the mode pair. The sum of $f_{wn,\langle.\rangle}$ of the mode pair, also indicated in Figure 4, is always 1, while the sum of $f_{dn,\langle.\rangle}$ is R_m. The total effective mass included in the analysis, if both modes of the mode pair are used (denoted by $M_{n,LU}$), can hence be given by

$$M_{n,LU} = \sum \mathbf{1}^{\mathrm{T}}\boldsymbol{s}_{n,\langle.\rangle} = \mathbf{1}^{\mathrm{T}}\boldsymbol{s}_{wn}\sum\left(f_{wn,\langle.\rangle}+f_{dn,\langle.\rangle}\right) = (1+R_m)M_{wn} \tag{34}$$

where the summation is taken over the n^{th} mode pair and $M_{wn} = \mathbf{1}^{\mathrm{T}}\boldsymbol{s}_{wn}$ is the effective modal mass of the original mode. The ratio of the modal mass included in the analysis to the total seismic mass of the structure is

$$\frac{M_{n,LU}}{\mathbf{1}^{\mathrm{T}}(\boldsymbol{m}_w+\boldsymbol{m}_d)\mathbf{1}} = \frac{(1+R_m)M_{wn}}{\mathbf{1}^{\mathrm{T}}\boldsymbol{m}_w(1+R_m)\mathbf{1}} = \frac{M_{wn}}{\mathbf{1}^{\mathrm{T}}\boldsymbol{m}_w\mathbf{1}} \tag{35}$$

The significance of Equation 35 becomes clear by recognising that the right hand side of the equation expresses the proportion of the n^{th} modal mass of the uncoupled in-plane wall to its total seismic mass. Equation 35 therefore states that the mode pair retains the same proportion of the modal mass of the combined structure as that of the original mode. This property is particularly attractive for low-rise URM buildings, for which the uncoupled in-plane wall's behaviour is likely to be dominated by its fundamental mode. This leads to the concept of the two-mode analysis, whereby the response of the structure is approximated by the mode pair (defined by Equations 25, 26, 28 and 29) corresponding to the fundamental mode of the uncoupled in-plane wall. The applicability of this two-mode analysis concept is evaluated for more general diaphragm configurations in the next section.

SENSITIVITY ANALYSIS

Parameters Investigated

The validity of the assumptions and the errors inherent in the two-mode analysis approach is evaluated through a sensitivity analysis, by varying the number of storeys, characteristics of the input excitation, the reference mass ratio and the period of the diaphragms, as well as the variations introduced in the diaphragm configuration.

Two, three and four storey models are considered, with the reference fundamental periods of the uncoupled in-plane wall (T_w) corresponding to 0.178 s, 0.241 s and 0.3 s respectively. These period values are calculated based on the empirical period formula of AS 1170.4 [16]

$$T_{rig} = 0.0625h^{0.75} \tag{36}$$

where h is the height of the building, calculated assuming all storey heights to be 3.2 m. As T_{rig} applies to rigid diaphragm structures, T_w is obtained by eliminating the mass attributed to the diaphragms. For simplicity, it is considered that an equal amount of mass is attributed to the diaphragms (representing the mass of the out-of-plane loaded walls) and the in-plane wall, such that

$$T_w = \frac{T_{rig}}{\sqrt{2}} \tag{37}$$

The tributary mass of the in-plane wall is set to 10 tons at all levels except at the roof, where it is halved to approximate the reduction in the tributary height. It should be noted that the magnitude of the mass has no effect on the displacement responses of classically damped systems, if the damping is specified as a fraction of the critical damping value for each mode. The stiffnesses of the in-plane walls are adjusted so that the fundamental mode shape of the uncoupled in-plane wall is linear in all cases.

The *reference* diaphragm condition consistent with Equations 16 and 17 is determined by the *reference mass ratio R_m* and the *reference diaphragm period T_d*. The variations in these parameters are independently controlled by ε_m and ε_T respectively. Four different variation profiles are considered, as shown in Figure 5. The figure shows the profiles for the positive ε_m variation as applied to a three storey model. Similar variations are investigated for the diaphragm periods, by the parameter ε_T. For the linear and the alternating profiles,

Table 1. List of natural accelerograms.

Event	Station	Year	Mw	Closest distance (km)	NEHRP site class	Scaling factor
Superstition Hills	Plaster City	1987	6.7	21	D	2.2
Northridge	Canoga Park - Topanga Can	1994	6.7	15.8	D	1.2
Northridge	N. Hollywood - Colwater Can	1994	6.7	14.6	C	1.7
Loma Prieta	Gilroy Array # 4	1989	6.9	16.1	D	1.3
Cape Mendocino	Rio Dell Overpass - FF	1992	7.1	18.5	C	1.2
Landers	Yermo Fire Station	1992	7.3	24.9	D	2.2

the reference values equal the average configurations of the diaphragms. For the top variation and the bottom variation profiles, all but one level have the reference values. The parameters ε_m and ε_T are varied independently from −0.5 to 0.5. The reference mass ratio R_m is varied from 0.5 to 2, and the diaphragm period T_d from 0.1 s to 2 s. These values are considered to encompass the likely range of parameters for typical existing URM buildings with timber diaphragms.

Acceleration Records

The sensitivity of the two-mode analysis to the input spectral shape is assessed by considering two sets of acceleration records. The first set consists of six natural accelerograms selected from the CUREE testing protocol [17] as scaled by [18]. As listed in Table 1, these records were measured in California on stiff soil (NEHRP site class C and D). The second set consists of artificial accelerograms compatible with AS 1170.4 on rock sites [19], which exhibit the dominance of high frequency content typical of intraplate regions. The mean pseudo-acceleration spectra of the two sets of records are shown normalised to their peak ground accelerations in Figure 6.

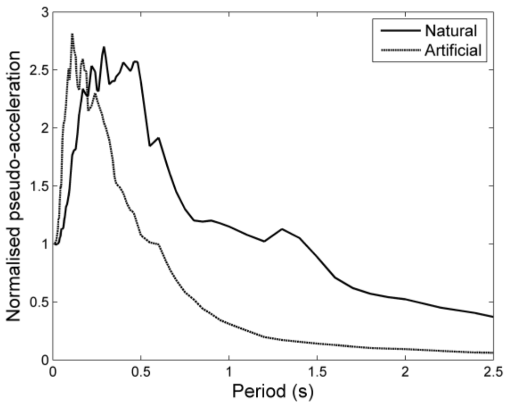

Figure 6: ***Comparison of the mean spectra of two sets of records.***

Analysis Procedure

For each parameter combination, two analyses are conducted. The first analysis is performed with the actual configuration of the diaphragms, including the variations in the mass ratio and the period. The time-history responses are calculated by Newmark's constant average acceleration method (γ = 0.5 and β = 0.25), with a constant damping ratio of 5% applied to all modes. The second analysis is carried out by using the reference values of diaphragms, R_m and T_d, and the mode pair corresponding to the fundamental mode of the uncoupled in-plane wall. For each mode, modal time-history displacements are solved and are superimposed to obtain the combined response of the mode pair. A constant damping ratio of 5% is also used in the second set of analyses to eliminate the influence of damping in the comparison of results.

Response Parameters

The two-mode analysis is evaluated based on the mean peak base shear and the interstorey drift of the in-plane wall. These are considered to represent the global and the local parameters most applicable in assessing the response of a building. Furthermore, the results are reported by the ratios of the mean peak responses (denoted generically as r) from the two-mode analysis (r_{est}) to the complete analysis (r_{act})

$$r = \frac{r_{est}}{r_{act}} \tag{38}$$

Error in Base Shear Estimation

The accuracy of the base shear estimation is found to depend on the flexibility of the diaphragms. In Figure 7, the range of the base shear ratios (Equation 38) for the four-storey model with ε_T of −0.3 is shown as a function of the period ratio, $R_T = T_d / T_w$. The plot shows the typical sensitivity characteristics observed, and includes all variation profiles. As shown in the figure, the two-mode analysis produces accurate results when the diaphragms become very flexible. The negligible influence of the very flexible diaphragms implies the in-plane wall to respond independent of the diaphragms. The largest error is generally observed when R_T is between 1 and 4, suggesting that the diaphragms have the most potential to modify the response of the in-plane wall when they are neither very stiff nor overly flexible.

The reference mass ratio shows no consistent influence on the maximum error in the estimation of the base shear. However, larger R_m typically results in larger errors in the flexible diaphragm range, approximately for $R_T > 4$.

No significant differences in the maximum error are observed for the two sets of input accelerograms. However, the natural accelerograms tend to result in larger errors in the range $R_T >$ 4.

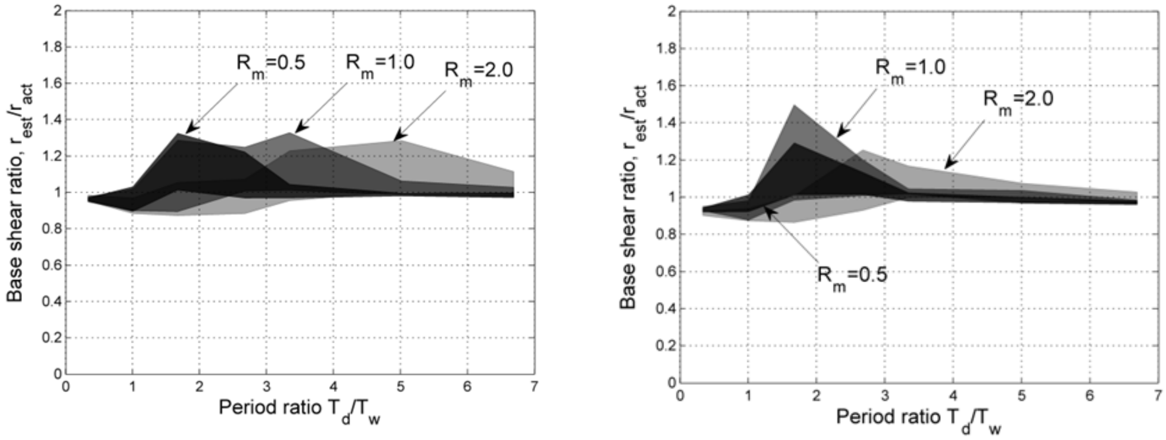

(a) Natural accelerograms *(b) Artificial accelerograms*

Figure 7: Ratio of mean peak base shear of the two-mode analysis to the actual results for four-storey model with ε_T of −0.3.

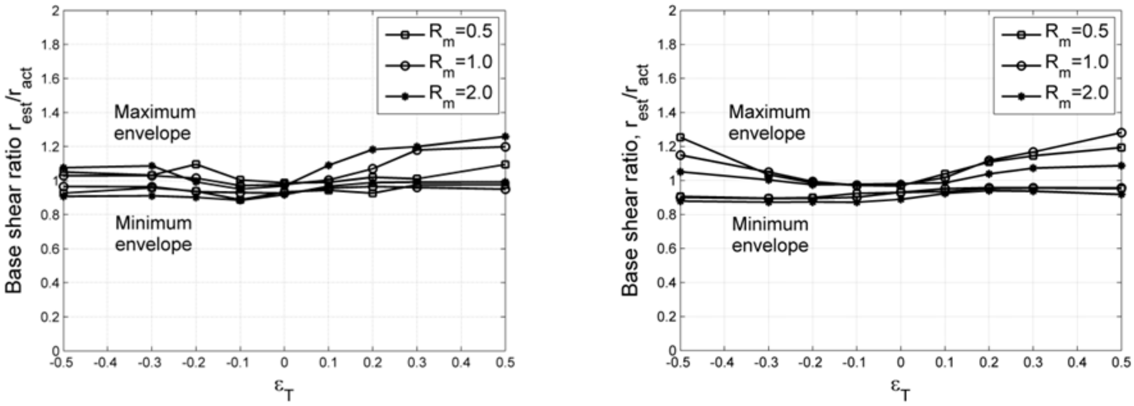

(a) Two-storey model *(b) Four-storey model*

Figure 8: Envelope of mean peak base shear ratio of top variation in ε_T for natural accelerograms.

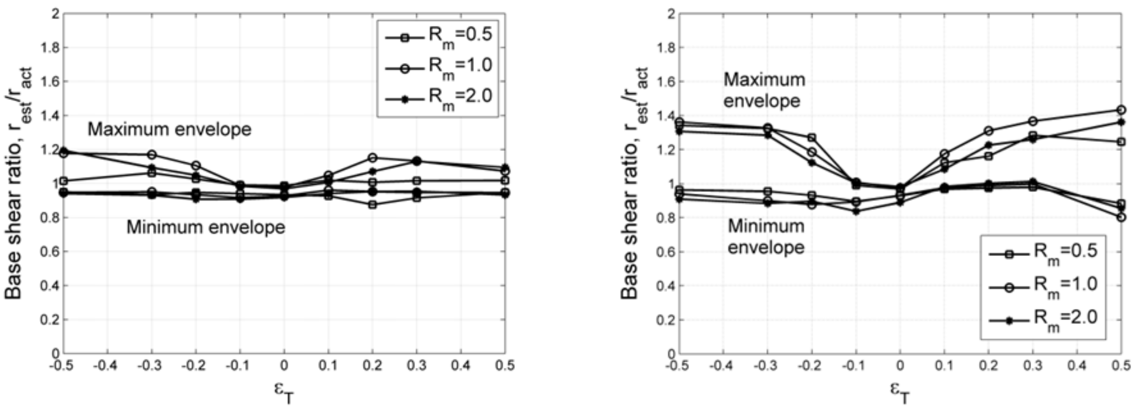

(a) Two-storey model *(b) Four-storey model*

Figure 9: Envelope of mean peak base shear ratio of linear variation in ε_T for natural accelerograms.

The envelopes of the maximum and the minimum base shear ratios are shown in Figure 8 for the top variation and in Figure 9 for the linear ε_T variation profiles for the natural accelerogram records. While not shown, similar results are obtained for the artificial accelerograms. The errors resulting from the variations in ε_m are also found to be similar to those of ε_T. Furthermore, results for the bottom variation and the alternating variation profiles are similar to those obtained for the top variation profile. As Figure 8 and Figure 9 show, the linear variation results in the largest error of the two-mode analysis. While the errors in the other variation profiles are insensitive to the number of storeys, the error for the linear variation grows with the number of storeys.

For the top, bottom and alternating variation profiles, the error in the base shear estimation using the two-mode analysis can be limited to ±20% if ε_m and ε_T are within ±30% of the reference values. For the linear variation, up to +40% error can be observed for the four-storey structures by keeping ε_m

and ε_T to within ±30% of the reference values. In general, there is a tendency for the two-mode analysis to overestimate the actual base shear. This may be attributed to the assumption of the equal diaphragm period inherent in the two-mode analysis, as this assumption results in the perfect correlation of the inertial forces transferred from the diaphragms to the in-plane wall.

Error in Interstorey Drift Estimation

The two-mode analysis generally results in larger errors in the interstorey drift estimation in comparison to the base shear.

For the top and the linear variation profiles, the variation in ε_m results in larger errors than the variation in ε_T, while for the bottom and the alternating variation profiles, ε_m and ε_T lead to similar levels of errors. This finding is shown in the ratios of the interstorey drifts of the bottom and linear variation profiles for the four-storey model, corresponding to ε_T (Figure 10) and ε_m (Figure 11). While not shown, the maximum error envelope of the top variation profile is similar to that of the linear variation profile, while the alternating variation profile tends to be between the bottom and the top variation profiles.

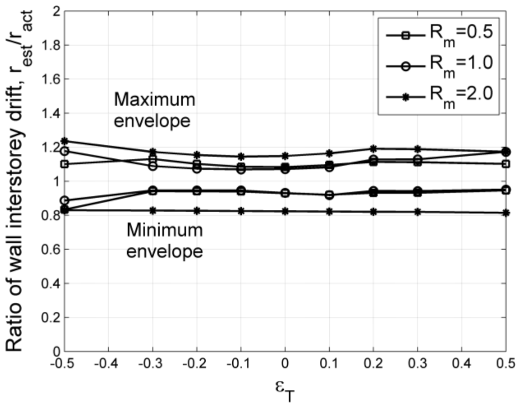

(a) Bottom variation profile

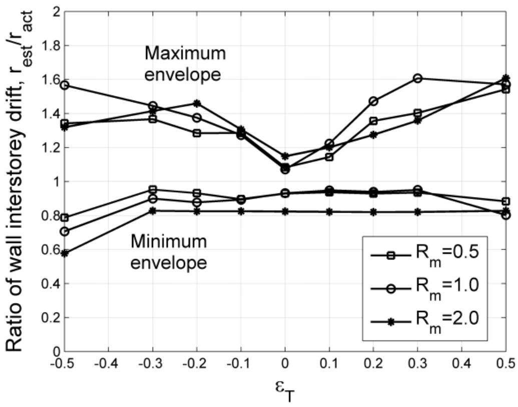

(b) Linear variation profile

Figure 10: ***Envelope of ratios of mean peak interstorey drift for four-storey model with variation in ε_T for natural accelerograms.***

From Figure 11, the two-mode analysis can be seen to produce conservative results when the mass ratio of the top level is less than the reference value (ε_m < 0), while noticeable underestimations may result when the top level has larger mass ratio (ε_m > 0). These observations have been consistently found for the top and the linear variation profiles, for both sets of accelerograms.

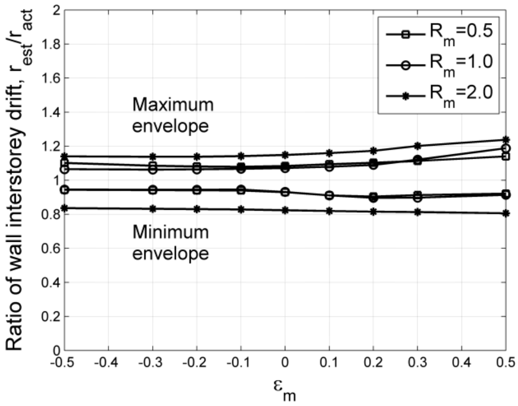

(a) Bottom variation profile

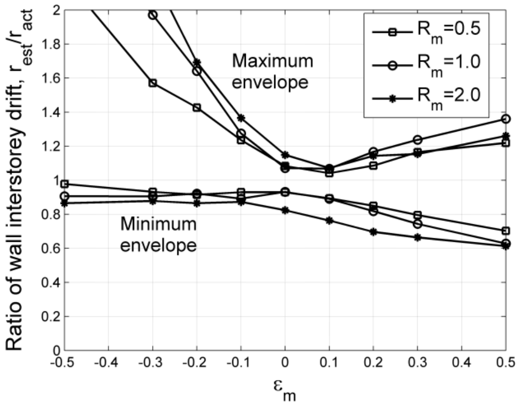

(b) Linear variation profile

Figure 11: ***Envelope of ratios of mean peak interstorey drift for four-storey model with variation in ε_m for natural accelerograms.***

The estimation of the interstorey drift can also be somewhat sensitive to the spectral shape of the excitation. The artificial accelerograms appear to induce larger participation of higher modes that are not considered in the mode pair analysis. This is seen in Figure 12, in which a constant level of error persists even for very flexible diaphragms.

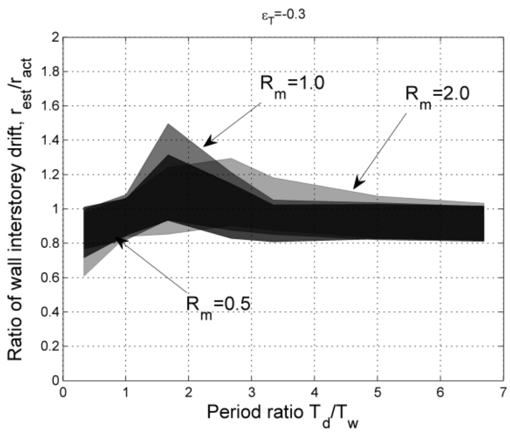

Figure 12: ***Ratio of mean interstorey drifts of the two-mode analysis to the actual results for four-storey mode with ε_T of −0.3.***

For buildings of up to three storeys, the error can be limited to between approximately −20% and +40% if ε_T is within ±30% of the reference value. For the four-storey models, an error of up to +60% may be obtained under the same condition. The variation in ε_m leads to even larger errors. For buildings of up to three storeys, errors between −20% and +60% are obtained for the bottom and the alternating variation profiles, if ε_m is within ±30% of the reference value. For the top and the linear variation profiles, the upper-bound errors increase to +90%. When the four-storey models are considered, significant overestimations (>100%) and underestimations (−60%) may be obtained.

The two-mode analysis appears to be appropriate in estimating the mean peak base shear of a structure with flexible diaphragms within the range of parameters investigated. However, the estimations of the local parameters, such as interstorey drifts, can become rather poor. It is envisaged that improved predictions of local demands can be achieved by modifying the mode shape assumed in the two-mode analysis.

Recommended Use of Two-mode Analysis

From the sensitivity analysis, the following criteria are suggested for application of the two-mode analysis:

- the number of storey to be limited to three;
- the variation profile should be selected so that ε_m and ε_T are minimised, and within approximately ±0.3;
- the bottom variation profile is the most favourable for both ε_m and ε_T, followed by the alternating, top and linear profiles; and
- for conservative estimates, the mass ratio of the topmost level to be smaller than the reference value R_m, if the top or the linear variation profile is used.

These condition are aimed at limiting the error in the mean peak base shear estimations to ±20%, while eliminating the excessive errors observed for the interstorey drift predictions.

APPLICATION TO LINEAR STATIC PROCEDURE

An improvement to the linear static procedure is proposed by utilising the finding that the two-mode analysis can generally provide reasonable predictions of the mean peak base shear. Expressions for the mode pair to be used in the method are firstly summarised. A coefficient that captures the effect of diaphragm flexibility on the base shear (base shear modification factor) is then derived analytically.

Formulae for Mode Pair

The mode pair corresponding to the fundamental mode is used in the linear static method. For the uncoupled in-plane wall with the fundamental period T_w, the periods of the mode pair (from Equations 25 and 26) can be written as

$$T_1 = T_w \left(\frac{2R_T^2}{R_T^2 + (1+R_m) - \sqrt{\left[R_T^2 + (1+R_m)\right]^2 - 4R_T^2}} \right)^{0.5} \qquad (39)$$

$$T_2 = T_w \left(\frac{2R_T^2}{R_T^2 + (1+R_m) + \sqrt{\left[R_T^2 + (1+R_m)\right]^2 - 4R_T^2}} \right)^{0.5} \qquad (40)$$

where $R_T = T_d / T_w$ is the reference period ratio and R_m is the reference mass ratio. The scaling factors (Equation 33) of the effective earthquake force distribution are also given in an alternative dimensionless form as

$$f_{wi} = \frac{1+R_m\beta_i}{1+R_m\beta_i^2},\ f_{di} = R_m\beta_i f_{wi},\ i = 1,2 \qquad (41)$$

where

$$\beta_i = \frac{T_i^2}{T_i^2 - (R_T T_w)^2},\ i = 1,2 \qquad (42)$$

Base Shear Modification Factor

The base shear modification factor, that expresses the effect of the flexible diaphragms on the peak base shear of the uncoupled in-plane wall, is herein derived analytically. Firstly considering the uncoupled in-plane wall, any peak response in the fundamental mode (denoted by r_w') can be written as [13]

$$r_w' = r_w'^{st} S_a(T_w) \qquad (43)$$

where $r_w'^{st}$ is the static response of the wall subjected to $\boldsymbol{s}_w$, as defined in Equation 31 for the uncoupled in-plane wall, and S_a is the ordinate of the pseudo-acceleration spectrum at the fundamental period of the uncoupled in-plane wall.

For linearly elastic structures, a proportionality exists between the applied force and the response,

$$r_w'^{st} \propto \boldsymbol{s}_w \qquad (44)$$

Using the expression of Equation 32, similar proportionality can also be written for the in-plane wall in the combined structure

$$r_{wi}^{st} \propto (f_{wi} + f_{di})\boldsymbol{s}_w,\ i = 1,2 \qquad (45)$$

where f_{wi} and f_{di} can be obtained from Equation 41. Because the proportionality in Equations 44 and 45 is governed by the stiffness of the in-plane wall, which is identical in the uncoupled and the combined systems, the two expressions imply

$$r_{wi}^{st} = (f_{wi} + f_{di}) r_w'^{st},\ i = 1,2 \qquad (46)$$

The peak dynamic in-plane wall's response in the combined structure r_w can then be approximated by the square-root-of-sum-of-squares (SRSS) combination of the mode pair, because the modes are widely spaced (see Figure 2),

$$r_w = r_w'^{st} \sqrt{\sum_{i=1}^{2} \left[(f_{wi} + f_{di}) S_a(T_i)\right]^2} \qquad (47)$$

where T_i is obtained from Equations 39 and 40. By specialising the response parameter to the base shear, the base shear modification factor is defined by

$$C_B = \frac{V_b}{V_b'} = \frac{\sqrt{\sum_{i=1}^{2} \left[(f_{wi} + f_{di}) S_a(T_i)\right]^2}}{S_a(T_w)} \qquad (48)$$

where V_b is the approximated base shear of the combined structure and V_b' is the base shear of the uncoupled in-plane wall. Hence by knowing the base shear of the uncoupled in-plane wall, the base shear of the combined structure accounting for the diaphragm vibration is given by

$$V_b = C_B V_b' \qquad (49)$$

Calculation of $\boldsymbol{T_w}$

In evaluating Equations 39 and 40, the fundamental period of the in-plane wall is required. Several options are available to calculate T_w:

- The in-plane wall may be modelled using frame elements with rigid offsets at nodal regions. Eigenvalue analysis can then be conducted. This approach option requires the use of software.

- The stiffness of the solid walls may be calculated using the mechanics for homogeneous materials, considering both the shear and the flexural deformations. For walls with openings, the wall stiffness may be obtained from the individual stiffnesses of piers by assuming appropriate boundary conditions. The typical common assumptions on the boundary condition are (1) strong pier - weak spandrel (i.e. cantilever piers), or (2) weak pier - strong spandrel (i.e. each pier in double bending). Once the wall stiffness is calculated, the Rayleigh's method [1] may be used to obtain the fundamental period.

Alternatively, the estimation of T_w may be avoided completely if a simplified analysis method is used, as described in the following section.

Simplified Method

The calculation of T_w admittedly involves a large approximation, especially if a wall stiffness is estimated from the individual pier stiffnesses. The sensitivity of the modified base shear (Equation 49) to variations in T_w is therefore investigated. Figure 14 shows a contour plot of V_B (as normalised to the weight of the structure), against the uncoupled in-plane wall period and the diaphragm period. The plot is generated from the expressions in Equations 39 to 49, using the design spectrum of NZS 1170.5 [20] on site subsoil class B (Figure 13), with the peak ground acceleration of 0.22 g. The mass ratio is set to 1. The transition periods of the design spectra are denoted as T_B and T_C as shown in Figure 13. These periods are also indicated in Figure 14. It can be observed that for a given value of T_d, the base shear is rather insensitive to variations in T_w. Furthermore, a reasonable conservative estimate can be made by setting $T_w = T_B$ for the typical period range of interest for URM buildings with flexible diaphragms (small T_w and moderate to large T_d). Consistent observations were made for other soil types and mass ratios. Hence a simplification is suggested for a practical application, by setting $T_w = T_B$.

In order to facilitate the use of the simplified method, the values of base shear modification factor (C_B) corresponding to $T_w = T_B$ are provided in Appendix B for the design spectra of NZS 1170.5. It is notable that C_B reduces with the increasing diaphragm flexibility. This suggests that the multi-mode behaviour associated with diaphragm flexibility leads to a general reduction in the base shear.

Note that the charts are developed using design spectra corresponding to the modal and time-history analyses (as opposed to the equivalent static analysis). This is because the spectra corresponding to the modal and time-history analyses reflect the hazard spectra, while those of the equivalent static analysis contain a cut-off period associated with the uncertainty involved in the estimation of short fundamental periods [21]. However, accounting for such uncertainty does not seem appropriate in the proposed method.

Once T_d and R_m are calculated, these charts can be read off to obtain the value of the modification factor corresponding to the site subsoil class of interest. This avoids the need to calculate T_w. The base shear of the uncoupled in-plane wall can be obtained using the peak ordinate of the design spectra. It should be noted, however, that this simplified method is to be used only in conjunction with smooth design spectra, and not with individual earthquake records.

Analysis Steps

The proposed linear static method consists of the following steps, applicable to essentially symmetric structures of up to three storeys in height:

1. Calculate the tributary masses of the in-plane wall and the diaphragms.

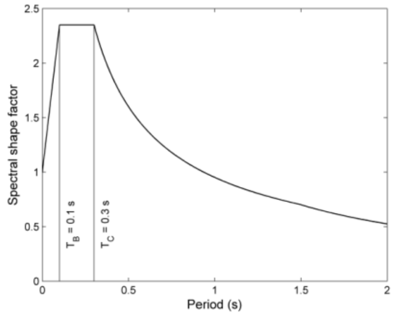

Figure 13:* *Design spectral shape factor of NZS 1170.5 for site subsoil class B.

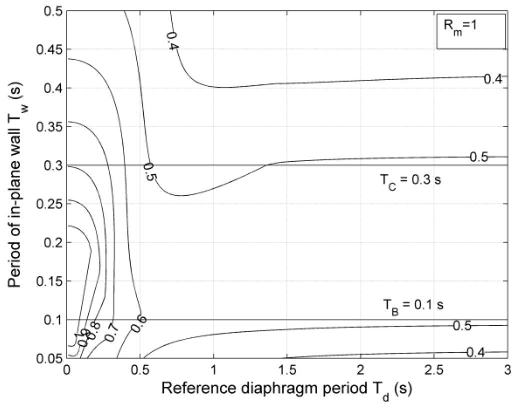

Figure 14:* *Contour plot of V_B (Equation 49).

2. Multiply the tributary masses of the diaphragms by 126/155 (Equation 5) to obtain the *effective* masses of the diaphragms. Calculate the mass ratio by dividing the effective diaphragm mass by the tributary mass of the in-plane wall at each level. Calculate the reference diaphragm mass ratio, R_m by selecting an appropriate variation profile of Figure 5, ensuring that ε_m is within ±0.3.
3. Calculate the periods of the diaphragms (Equation 4, also refer [4, 22]) and the reference diaphragm period T_d by selecting an appropriate variation profile of Figure 5 (by replacing R_m and ε_m of Figure 5 by T_d and ε_T respectively), ensuring that ε_T is within ±0.3. Note that the variation in T_d does not need to assume the same profile as that of R_m.
4. Calculate the fundamental period (T_w) and the mode shape (ϕ) of the uncoupled in-plane wall. Alternatively, the simplified method can be used, by assuming $T_w = T_B$.
5. Calculate C_B from Equation 48, using the associated expressions in Equations 39 to 42. If the simplified method is used, C_B may be read off from one of the charts provided in Appendix B.
6. Calculate the peak base shear of the uncoupled in-plane wall (V_B'), by multiplying the seismic mass of the in-plane wall by $S_a(T_w)$, where S_a is the ordinate of the pseudo-acceleration spectrum. If the simplified method is used, the peak ordinate of the spectrum should be used.
7. In order to account for the inelastic deformation, the base shear may be further modified, for example, by C_1, C_2 and C_m of Equation 1. However, further studies are needed to confirm the validity of these coefficients for structures with flexible diaphragms.
8. The equivalent lateral forces on the in-plane walls are obtained by distributing the modified base shear in

proportion to $m_j\ \phi_j\ /\sum\ m_i\ \phi_i$ for the j^{th} level. If the simplified method is used, ϕ may be approximated by the floor heights from the ground (linear variation), as typically specified in codes [1, 16, 20]. This approximation is consistent with the assumption of the first-mode dominance of the in-plane wall used in the two-mode analysis.

9. The resulting member forces (which can be evaluated using an equivalent frame model, or determined on the basis of the relative stiffnesses of the piers and spandrels) are compared to their capacities, for example using Equation 2.

Analysis Effort

The effort needed to carry out the proposed method is comparable to existing methods. This section provides the comparison of the analysis procedures of two existing methods, ASCE 41-13 and a method by Knox [6], and the approach proposed in this study. The overview of the existing methods is provided in Appendix A. The following can be noted:

- All methods require the calculations of tributary masses and the diaphragm period of each span at each floor level. Hence the analysis steps 1 and 3 of the preceding section are identical for all methods.
- Analysis step 2 is unique to the proposed method. However, this step requires minimal effort.
- The calculation of the uncoupled in-plane wall period (step 4) is required in the rigorous version of the proposed method and in the method by Knox. However, as described previously, the simplified approach can be used to eliminate the need to compute the fundamental period of the wall.
- The calculation of C_B in step 5 is unique to the proposed method. However, this step requires minimal effort, especially if the simplified approach is used.
- ASCE 41-13 and Knox's methods require the computation of the equivalent static force for each diaphragm, while the proposed method requires the equivalent static force of the in-plane wall only.
- Knox's method requires the calculation of base shear by complete quadratic combination (CQC) of the diaphragm forces and the in-plane wall force to avoid the potential underestimation of storey forces obtained by SRSS. This may require certain additional effort in calculating the correlation coefficients.

The steps 7 onwards are identical in all methods. The foregoing discussion confirms that the effort needed to conduct the proposed method is comparable to the existing methods.

Numerical Validation

A two-storey symmetric building shown in Figure 15 is analysed using the proposed method. In addition, ASCE 41-13 and the method by Knox are also evaluated for comparison. In this validation, the rigorous version of the method is used with the "actual" uncoupled in-plane wall period obtained from the modal analysis of the wall modelled by frame elements and rigid offsets. In addition, only the elastic response is evaluated, because the modification for the inelastic response is in principle identical for all methods.

In the analysis, the loading is considered in the direction parallel to walls 1 and 2, and perpendicular to the floor and roof joists. The out-of-plane walls (walls 3 and 4) are solid with no openings. The thicknesses of the walls are 350 mm in the first storey and 230 mm in the higher levels. The density of masonry is 1800 kg/m^3 and the Young's modulus is 2750 MPa. The shear modulus is assumed to be 40% of the Young's modulus.

Using an equivalent frame model, the fundamental period of the in-plane wall is calculated to be 0.097 s. The mode shape is 0.478 at the first floor and 1.0 at the roof level, indicating an almost linear profile. The effective mass of the fundamental mode is 85% of the total mass of the in-plane wall.

Three different diaphragm constructions are considered. The diaphragm stiffnesses of the first two cases are calculated using the procedure outlined in [22]. The third case represents more heavily loaded stiff timber diaphragms.

In the first case (case 1), the first level diaphragm is considered to be in a "fair" condition and sheathed with single straight floor board, while the roof has single diagonal sheathing and is in a "poor" condition (see [22]). Using the procedure of [22], and neglecting for simplicity the effects of floor opening and additional stiffness of the out-of-plane wall, the diaphragm stiffness G_d is calculated to be 215 kN/m at the first floor and 340 kN/m at the roof. Assuming 18 mm thick sheathing and 55 mm by 240 mm deep joists spaced at 405 mm centres, with the timber density of 610 kg/m^3, the self-weight of the floor is calculated to be 0.3 kPa. The self-weight of the roof is considered to be 0.6 kPa, accounting for an additional 0.3 kPa for the roofing. The floor is also subjected to an additional 0.9 kPa (3 kPa imposed load multiplied by the seismic load factor of 0.3) imposed load.

In the second case (case 2), the floor diaphragm is considered to have been strengthened with blocked 9 mm plywood overlay (unchorded), increasing G_d to 1460 kN/m. The roof is also strengthened with an additional layer of diagonal sheathing, resulting in G_d of 2385 kN/m. In addition, the self-weight of the floor and the roof increase to 0.36 kPa and 0.72 kPa respectively, due to the additional strengthening material.

The third case (case 3) represents a more heavily stiffened case in which the floor and the roof diaphragms have the same stiffness G_d of 3150 kN/m. This value represents the upper-bound expected stiffness of timber diaphragms in ASCE 41-13. The dead load of the floor and the roof are considered to be 1.5 kPa, taken as an average value reported for a two-storey building by [23], which contains large mass contributions from the ceiling and wood partitions. In addition, a 1.5 kPa imposed load is considered for the floor (5 kPa live load with the seismic load factor of 0.3).

The calculated diaphragm mass ratio and periods are shown in *Table 2* for the three cases. In this example, the linear profile has been chosen for both parameters, resulting in the reference parameters R_m and T_d being the average values of the mass ratios and the diaphragm periods. The values of ε_m and ε_T can then be calculated from Figure 5. For example, using the first floor mass ratio of 0.425 and the reference R_m of 0.457 for case 1 (see Table 2), the value of ε_m is obtained by substituting the above values in the expression given in Figure 5 for the linear profile; i.e. $0.457(1-\varepsilon_m)=0.425$, resulting in ε_m of 0.07.

The calculated values of ε_m are 0.071, 0.089 and 0.029 respectively for the first, second and the third cases. Similarly, the values of ε_T are -0.22, -0.21 and -0.12 respectively for the three cases. It is noted that all ε_m and ε_T values are within the suggested limit of ±0.3.

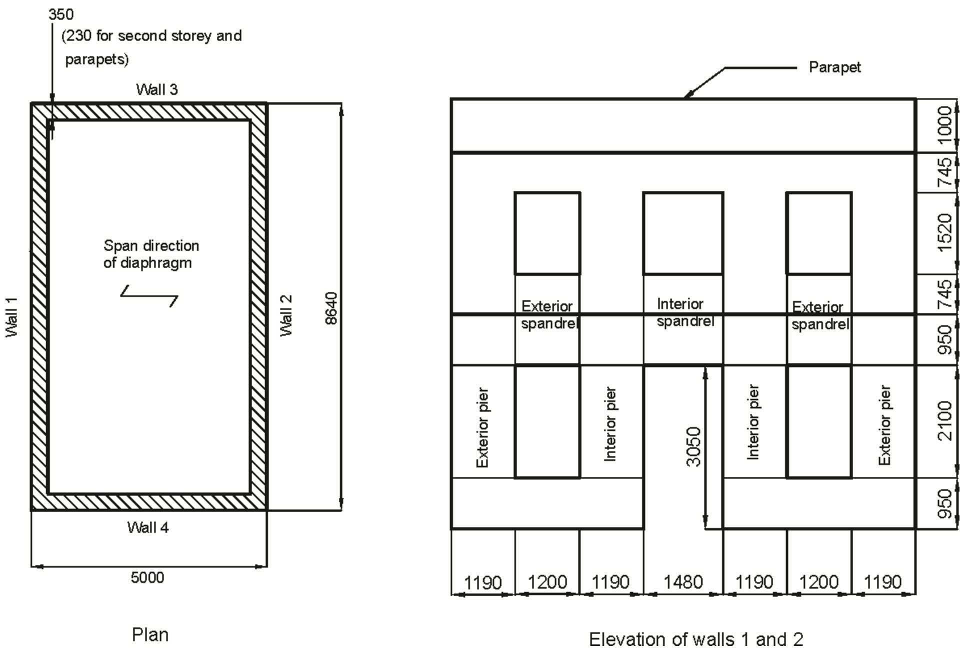

Figure 15: Example structure.

The structures are analysed with the proposed method using the mean spectrum of the natural records listed in Table 1. In order to assess the accuracy of the method, linear dynamic analyses are conducted in SAP2000 [24] using the six accelerograms. The in-plane walls are modelled as equivalent frames with rigid offsets, while the diaphragms are modelled by beam elements with artificially large bending stiffness to simulate the shear deformation compatible with Equation 4. In addition, the existing linear static method by Knox, as well as the method contained in ASCE 41-13 for URM buildings with flexible diaphragms, are also evaluated. In the ASCE 41-13 method, the updated diaphragm period expression of Equation 4 by [4] is used. In all analyses, a constant modal damping ratio of 5% is used. The results from the three linear static methods are compared against the time-history results.

Table 3 shows the predicted mean peak moments of the in-plane wall elements, indicated in Figure 15 for the first storey, as normalised to the dynamic analysis results for case 1. Similar results are shown in Table 4 and Table 5 for case 2 and 3 respectively. The comparison shows that the proposed and the Knox's methods produce comparably good predictions of the dynamic results for the flexible diaphragms in case 1. The method of ASCE 41-13, however, results in large overestimations. When the diaphragm stiffness is increased in case 2, the proposed method reports the same level of accuracy as in case 1, while Knox's method results in some underestimations. The overestimation of ASCE 41-13 reduces, although the method is still overly conservative. For the most stiff and heavy diaphragms of case 3, the proposed method provides reasonably consistent results with the dynamic analysis, while Knox's method results in further hand, underestimations. The method in ASCE 41-13, on the other hand provides a comparable level of accuracy to that as the proposed method.

It appears that the ASCE 41-13 is more suited to the analysis of structures when the diaphragms are relatively stiff, as this method assumes the total tributary mass to respond in a single period. Conversely, the method of Knox appears more suitable when the diaphragms are relatively flexible, as it treats the in-plane wall and the diaphragms to vibrate independently. In comparison to these existing procedures, the proposed method is capable of providing consistent predictions of seismic demand for a wide range of diaphragm stiffnesses.

Discussion on Inelastic Behaviour

The basic premise of the linear static procedure, when used in the performance-based assessment, is that the peak inelastic displacement can be estimated from the displacement of the corresponding elastic system. For example, the modification factor C_1 in Equation 1 accounts for the presumed difference between the peak inelastic displacement and the elastic displacements. In FEMA 356 [25] (and adopted by [6]), C_1 is given as 1.0 if the period of the structure is larger than the characteristic earthquake period (T_C) and as 1.5 if the building period is less than 0.1 s. Linear interpolation is allowed between these period values. In ASCE 41-13, a more elaborate expression is provided

$$C_1 = 1 + \frac{\mu_{strength} - 1}{aT^2} \tag{50}$$

where a is a factor that depends on the site subsoil classification, T is the fundamental period of the structure, and

Table 2: Diaphragm configuration (case 1: as-built; case 2: plywood overlay; case 3: heavily stiffened).

Level	Mass ratio (effective diaphragm mass / in-plane wall mass)			Diaphragm period (from Equation 4)		
	Case 1	**Case 2**	**Case 3**	**Case 1**	**Case 2**	**Case 3**
1	0.425	0.432	0.639	0.45 s	0.17 s	0.14 s
2	0.490	0.515	0.678	0.29 s	0.11 s	0.11 s
Average	0.457	0.474	0.658	0.37 s	0.14 s	0.13 s

$\mu_{strength}$ is the strength ratio defined by

$$\mu_{strength} = \frac{S_a}{V_y/W} \quad (51)$$

where V_y is the base shear capacity.

These expressions were derived from analytical and experimental investigations of earthquake response of yielding systems [1], considering the diaphragm to be rigid. It is beyond the scope of this paper to assess the adequacy of these expressions for structures with flexible diaphragms, which is an ongoing area of research activity at the University of Adelaide and the University of Auckland.

CONCLUSION

A method for the seismic analysis of in-plane loaded walls in a symmetric, low-rise building with flexible diaphragms has been presented. The method approximates the peak response of the in-plane walls using two modes of the structure assuming (1) equal ratio of diaphragm mass to the in-plane wall mass at all levels, and (2) equal diaphragm period at all levels. Under these conditions, the modal analysis has shown that two modes are typically sufficient to capture the majority of mass participation for regular low-rise buildings. Sensitivity analysis has been conducted to show that the two-mode analysis gives reasonable predictions of the base shear, even when the diaphragm configurations deviate from the assumed conditions. However, the predictions of interstorey drifts were less accurate, as the variations in the mass ratio and the period of the diaphragms resulted in modified mode shapes from those assumed in the two-mode analysis. Further studies are envisaged to address this issue.

An improvement to the linear static method has been proposed by utilising the two-mode analysis. Simple expressions are provided to capture the effect of flexible diaphragms. A simplified version of the method is also proposed to facilitate a rapid use of the procedure in practice. The proposed method provides an improvement to the existing procedures, as it explicitly considers the dynamic interaction between the in-plane wall and the diaphragms. The method has been shown to produce results consistent with dynamic analysis for a wide range of diaphragm stiffness values in the elastic range of building behaviour. Further studies are needed to assess the general suitability of the linear static procedure for URM buildings, and how the inelastic displacement should be obtained from the corresponding elastic system response when flexible diaphragms are present.

ACKNOWLEDGMENTS

The financial support for this work was provided by the Australian Federal Government through an Australian Research Council grant and an Australian Postgraduate Award.

Table 3: Peak moments from linear static methods normalised to mean peak dynamic results for case 1.

Element	Location	Proposed method		Method by Knox		ASCE 41-13	
		Storey 1	Storey 2	Storey 1	Storey 2	Storey 1	Storey 2
Pier	Exterior	1.13	1.29	1.25	1.08	2.41	1.99
	Interior	1.07	1.24	1.16	1.08	2.25	2.00
Spandrel	Exterior	1.27	1.26	1.33	1.11	2.54	2.04
	Interior	1.16	1.24	1.19	1.10	2.89	2.04

Table 4: Peak moments from linear static methods normalised to mean peak dynamic results for case 2.

Element	Location	Proposed method		Method by Knox		ASCE 41-13	
		Storey 1	Storey 2	Storey 1	Storey 2	Storey 1	Storey 2
Pier	Exterior	1.08	1.29	0.91	0.77	1.57	1.14
	Interior	1.03	1.23	0.85	0.78	1.45	1.14
Spandrel	Exterior	1.24	1.25	0.98	0.79	1.63	1.16
	Interior	1.14	1.22	0.87	0.79	1.43	1.17

Table 5: Peak moments from linear static methods normalised to mean peak dynamic results for case 3.

Element	Location	Proposed method		Method by Knox		ASCE 41-13	
		Storey 1	Storey 2	Storey 1	Storey 2	Storey 1	Storey 2
Pier	Exterior	0.95	1.22	0.69	0.63	1.11	0.92
	Interior	0.90	1.15	0.64	0.62	1.03	0.91
Spandrel	Exterior	1.07	1.19	0.73	0.64	1.16	0.94
	Interior	0.98	1.12	0.65	0.62	1.01	0.91

REFERENCES

1 ASCE (2013). "Seismic evaluation and retrofit of existing buildings". *ASCE/SEI 41-13*, American Society of Civil Engineers, Reston, Virginia.

2 Abrams, D.P. (2001). "Performance-based engineering concepts for unreinforced masonry building structures". *Prog. Struct. Engng Mater.*, **3**, 48-56.

3 NZSEE (2006). "Assessment and improvement of the structural performance of buildings in earthquakes". *New Zealand Society for Earthquake Engineering,* Wellington, New Zealand.

4 Wilson, A., Quenneville, P. and Ingham, J. (2013). "Natural period and seismic idealization of flexible timber diaphragms". *Earthquake Spectra*, **29**(3), 1003-1019.

5 Kim, S.-C. and White, D.W. (2004). "Linear static analysis of low-rise buildings with flexible diaphragms using the structural separation method". *Engineering Structures*, **26**, 83-93.

6 Knox, C. (2012). "Assessment of perforated unreinforced masonry walls responding in-plane". *Doctoral dissertation*. Department of Civil and Environmental Engineering, University of Auckland.

7 Fleischmann, R.B., and Farrow, K.T. (2001). "Dynamic behaviour of perimeter lateral-system structures with flexible diaphragms". *Earthquake Engineering and Structural Dynamics*, **30**, 745-763.

8 Lee, H.J., Aschheim, M.A. and Kuchma, D. (2007). "Interstory drift estimates for low-rise flexible diaphragm structures". *Engineering Structures*, **29**, 1375-1397.

9 Chen, Y. and Soong, T.T. (1988). "State-of-the-art review seismic response of secondary systems". *Engineering Structures*, **10**, 218-228.

10 Tena-Colunga, A. and Abrams, D.P. (1992). "Response of an unreinforced masonry building during the Loma Prieta earthquake". *Civil Engineering Studies – Structural Research Series No. 576*. Department of Civil Engineering, University of Illinois at Urbana-Champaign.

11 Kim, S.-C. and White, D.W. (2003). "MDOF response of low-rise buildings". *Final Report Project ST-5*.Mid-America Earthquake Research Center, Georgia Institute of Technology.

12 Sadashiva, V.K., MacRae, G.A., Deam, B.L. and Spooner, M.S. (2012). "Quantifying the seismic response of structures with flexible diaphragms". *Earthquake Engineering and Structural Dynamics*, **41**(10), 1365-1389.

13 Chopra, A.K. (2007). "Dynamics of structures – theory and applications to earthquake engineering". 3rd Edition. *Pearson Prentice Hall*, New Jersey.

14 Suarez, L.E. and Singh, M.P. (1987). "Seismic response of SDF equipment-structure system". *Journal of Engineering Mechanics*, **113**(1), 16-30.

15 Lay, D.C. (2003). "Linear algebra and its applications". 3rd Edition. *Pearson Education*.

16 Standards Australia (2007). "Structural design actions. Part 4: Earthquake actions in Australia". *AS 1170.4-2007. Standards Australia*, Sydney, Australia.

17 Krawinkler, H., Parisi, F., Ibarra, L., Ayoub, A. and Medina, A.R. (2000). "Development of a testing protocol for wood frame structures". *CUREE* Report Np. W-03. Richmond, CA.

18 Christopoulos, C., Filiatrault, A. and Folz, B. (2002). "Seismic response of self-centring hysteretic sdof systems". *Earthquake Engineering and Structural Dynamics*, **31**, 1131-1150.

19 Lam, N., Wilson, J. and Venkatesa, S. (2005). "Accelerograms for dynamic analysis under the new Australian Standard for Earthquake Actions". *Electronic Journal of Structural Engineering,* **5**, 10-35.

20 New Zealand Standard (2004). "Structural design actions Part 5: Earthquake actions - New Zealand". *NZS 1170.5:2004*. *Standards New Zealand*, Wellington, New Zealand.

21 New Zealand Standard (2004). "Structural design actions Part 5: Earthquake actions - New Zealand - Commentary". *NZS 1170.5 Supp1:2004*. *Standards New Zealand*, Wellington, New Zealand.

22 Giongo, I., Wilson, A., Dizhur, D, Derakhshan, H., Tomasi, R., Griffith, M., Quenneville, P. and Ingham, J. (2014). "Detailed seismic assessment and improvement procedure for vintage flexible timber diaphragms". *Bulletin of the New Zealand Society for Earthquake Engineering*, **47**(2), 97-118.

23 Bruneau, M. (1994). "Seismic evaluation of unreinforced masonry buildings - a state-of-the-art report". *Canadian Journal of Civil Engineering*, **21**(3), 512-539.

24 CSI (2012). SAP2000 v15. Computers and Structures Inc. Berkeley, CA.

25 FEMA (2000). "Prestandard and commentary for the seismic rehabilitation of buildings". *FEMA 356*. Federal Emergency Management Agency, Washington, D.C.

APPENDIX A - OVERVIEW OF EXISTING METHODS

ASCE 41-13

ASCE 41-13 contains a linear static procedure for unreinforced masonry buildings with single-span flexible diaphragms with six stories or less in height. In this procedure, the fundamental period is calculated as given in Equation 3. The peak static force for each diaphragm is then obtained as in Equation 1. The static force calculated for each diaphragm is then distributed to the in-plane walls in accordance with their tributary masses, and the design actions in each component is evaluated.

Knox

The method by Knox considers the uncoupled fundamental periods of the in-plane wall (T_w) and diaphragms (T_i) separately. T_w may be evaluated by modelling the wall using frame elements, and T_i is evaluated from Equation 4. Using the calculated period, the diaphragm force is evaluated as

$$V_{di} = C_1 C_3 S_a(T_i) W_D \tag{A3}$$

where W_D is the tributary weight of the diaphragm. The in-plane wall base shear is calculated by

$$V_w = C_1 C_3 S_a(T_w) W_w \tag{A4}$$

where W_w is the total weight of the in-plane wall. The coefficients C_1 and C_3 have been adopted from FEMA 356, and account for the inelastic behaviour and P-delta effects respectively. The in-plane wall's base shear from Equation A4 is distributed up the height of the wall in proportion to the tributary wall mass at the i^{th} level. The equivalent static force at the i^{th} level is then approximated by the SRSS combination of the diaphragm and in-plane wall forces,

$$V_{si} = \sqrt{\left(\frac{V_{di}}{2}\right)^2 + (V_{wi})^2} \qquad \text{(A5)}$$

where V_{wi} is the distributed in-plane wall's base shear.

In order to account for closely spaced modes, the total base shear is also evaluated by combining V_{di} and V_w using the complete quadratic combination (CQC) rule. If the sum of equivalent static forces calculated from Equation A5 is smaller than the base shear obtained using CQC, they are scaled up accordingly. Note that while the SRSS estimation may be carried out without calculating T_w, the CQC base shear check requires the periods of all components.

APPENDIX B - PLOTS OF C_B FOR SIMPLIFIED APPROACH

The plots of base shear modification factor C_B generated for the design spectra of NZS 1170.5 are provided in Figure B1 for different site subsoil classes. The plots correspond to $T_w = T_B$ and can be used to simplify the proposed method.

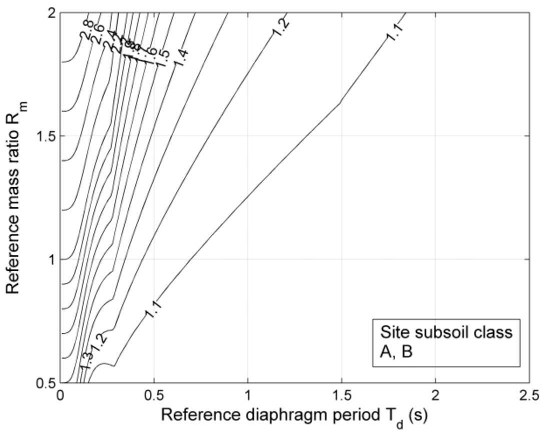

(a) C_B *for site subsoil class A or B*

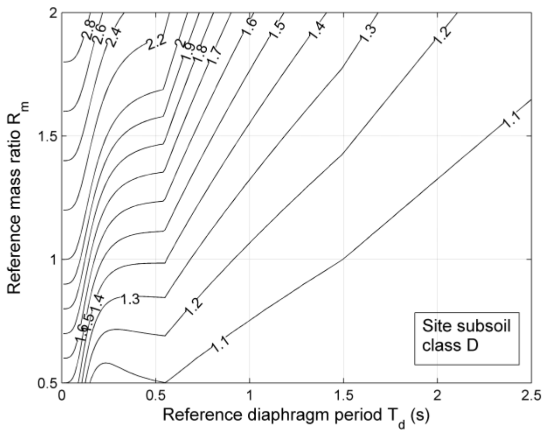

(c) C_B *for site subsoil class D*

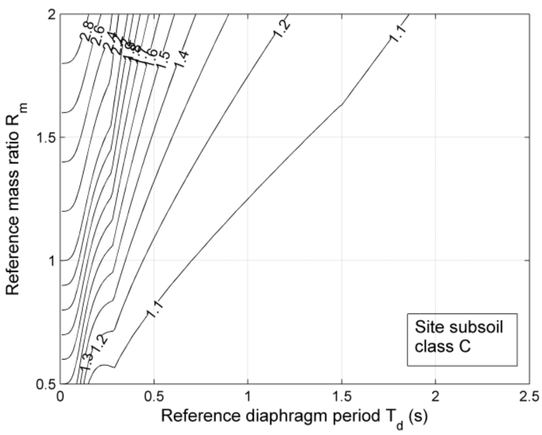

(b) C_B *for site subsoil class C*

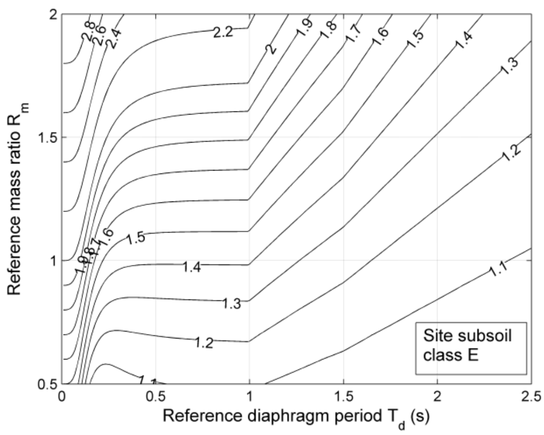

(d) C_B *for site subsoil class E*

Figure B1: Values of C_B for different site subsoil classes.